Chemotherapeutic Drugs Released from Polymers: Distribution of 1,3-bis(2-chloroethyl)-1-nitrosourea in the Rat Brain

Lawrence K. Fung,[1] Marian Shin,[1] Betty Tyler,[2] Henry Brem,[2,3] and W. Mark Saltzman[1,4]

Purpose. The distribution of [³H]BCNU following release from polymer implants in the rat brain was measured and evaluated by using mathematical models.

Methods. [³H]BCNU was loaded into p(CPP:SA) pellets, which were subsequently implanted intracerebrally in rats; [³H]BCNU was also directly injected into the brains of normal rats and rats with intracranially transplanted 9L gliomas. Concentrations of [³H]BCNU on coronal sections of the brain were measured by autoradiography and image processing. For comparison, the kinetics of [³H]BCNU release from the p(CPP:SA) polymer discs into phosphate-buffered saline were also measured.

Results. High concentrations of BCNU (corresponding to ~1 mM) were measured near the polymer for the entire 30-day experiment. The penetration distance, defined as the distance from the polymer surface to the point where the concentration of [³H]BCNU in the tissue had dropped to 10% of the maximum value, was determined: penetration distance was ~5 mm at day 1 and ~1 mm at days 3 through 14. Local concentration profiles were compared with a mathematical model for estimation of the modulus ϕ^2, an indicator of the relative rate of elimination to diffusion in the brain. From day 3 to 14, ϕ^2 was ~7, indicating that BCNU elimination was rapid compared to the rate of diffusive penetration into tissue. The enhanced penetration observed on day 1 appears to be due to convection of extracellular fluid caused by transient, vasogenic edema, which disappears by day 3.

Conclusions. Polymer implants produce very high levels of BCNU in the brain, but BCNU penetration into brain tissue is limited due to rapid elimination.

KEY WORDS: controlled release; brain tumor; polymer; diffusion; BCNU.

INTRODUCTION

Brain tumors are difficult to treat due to the presence of the blood-brain barrier. Interstitial delivery of chemotherapeutic agents using controlled release polymeric implants can bypass the blood-brain barrier, potentially providing high local concentrations of cytotoxic agents for sustained periods. The biocompatibility and safety of controlled release implants composed of p(CPP:SA) has been established (1–4). Furthermore, the

[1] Department of Chemical Engineering, The Johns Hopkins University, Room 24, New Engineering Building, 34th and Charles Streets, Baltimore, Maryland.

[2] Department of Neurosurgery, The Johns Hopkins School of Medicine, Baltimore, Maryland.

[3] Department of Oncology, The Johns Hopkins School of Medicine, Baltimore, Maryland.

[4] To whom correspondence should be addressed.

p(CPP:SA) implants containing BCNU improved survival in animals with experimental brain tumors (1, 4) and human patients with malignant glioma (4, 5). Still, the relationship between the rate of drug release from the polymer, local drug concentration in the tissue, and effectiveness against tumors is unknown.

Ninety percent of resected malignant gliomas recur within a 2-cm margin from the tumor (6). The anti-tumor agent must therefore migrate a sufficient distance from the polymer implant to treat recurrent tumor effectively. Previously, the release of [¹⁴C]BCNU or [³H]BCNU from polymers placed in brains of normal rats (7) and rabbits (8) was studied. However, these previous studies only measured regional distribution of the radiolabel, not local concentrations, making it difficult to correlate the dynamics of release from the polymer with drug distribution in the tissue.

In the present report, the spatial distribution of [³H]BCNU following controlled release by the p(CPP:SA) implant was quantified in several ways. The total amount of drug present in coronal sections and the local concentrations of the drug in the vicinity of the implant were measured over a 30-day period following implantation. Quantitative data were interpreted by comparison to models of BCNU transport and elimination within the brain interstitium. These models were then used to quantify the characteristics of release and transport in the normal rat brain, such as the rate of BCNU release from the polymer, diffusion coefficient and elimination constant of BCNU in the brain, and interstitial fluid velocity. For comparison, [³H]BCNU was injected in both normal and tumor-bearing brains, and the drug concentration profiles in both cases were compared. The kinetics of release of [³H]BCNU in phosphate-buffered saline were measured to compare with concentrations measured in brain interstitium.

MATERIALS AND METHODS

Animals and Cell Lines

Adult Fisher 344 male rats (7–8 weeks) were obtained from Harlan Sprague-Dawley, Inc. (Indianapolis, IN). All procedures in handling animals adhered to the "Principles of Laboratory Animal Care" (NIH publication #85-23, revised 1985). The 9L glioma was obtained from Marvin Barker, Brain Research Center, University of California, San Francisco. The culture of tumor cells and propagation of solid tumors were described elsewhere (9).

Materials

[³H]BCNU was synthesized in the Pharmacology Laboratory of The Johns Hopkins Oncology Center. Poly[bis(p-carboxyphenoxy)propane-sebacic acid] (20:80 w/w ratio) was kindly provided by Dr. Abraham Domb, Hebrew University, Jerusalem, Israel. The anesthesia solution contained 14.2 ml of ethanol (95%), 2.5 ml of xylazine (100 mg/ml, Rompun, Mobay Company, Shawnee, KS), 25 ml of ketamine hydrochloride (100 mg/ml, Parke-Davis, Morris Plains, NJ) and 58 ml sterile saline (0.9% NaCl). The solution was filter sterilized.

Fabrication of Drug-loaded Polymer

[³H]BCNU was encapsulated in p(CPP:SA) by solvent evaporation, as follows. Eight hundred milligrams of p(CPP:SA) copolymer was dissolved in 8 ml of methylene chloride. The solution was mixed with 200 mg of [³H]BCNU at room temperature. The homogeneous mixture was then transferred to a petri dish and kept in a vacuum desiccator overnight. Ten milligrams of the dried product was compressed under high pressure in a mold to fabricate a single wafer. The diameter and height of the polymer disc were 3 mm and 2 mm, respectively. Each disc contained about 2 mg of [³H]BCNU with 30 to 35 μCi of radioactivity.

In Vitro Release Study

The release of [³H]BCNU from the p(CPP:SA) disc was monitored during incubation in a phosphate-buffered saline solution (PBS: 120 mM NaCl, 2.7 mM NaCl, and 10 mM phosphate salts) at 37°C. Two polymer pellets were immersed separately in 5 ml of PBS at pH 7.4. At specific times following immersion, the PBS was replaced with fresh solution, and the radioactivity in the removed solution was determined by scintillation counting.

Direct Stereotactic Microinjection of [³H]BCNU into Normal Brain

Fisher 344 male rats were anesthetized with 0.6 to 0.7 ml of xylazine/ketamine administered intraperitoneally. A 3-cm incision was made and bregma was exposed. A 3-mm burr hole was drilled 1 mm anterior to the bregma and 3 mm lateral from the sagittal suture. The rat was placed in a stereotaxic frame and a cannula, which was connected to a 5-μl microsyringe (Hamilton, Reno, NV), was introduced into the brain parenchyma to a depth of 5 mm. The delivery of [³H]BCNU was initiated 2 minutes after the cannula was fully inserted. Each rat received a total volume of 2 μl (containing about 2 or 8 μCi) which was drawn from a solution comprising 2 mg [³H]BCNU in 16 μl of 95% ethanol solution. This was administered at a rate of 0.2 μl/min, which was controlled by a microinjection unit and a stopwatch. The cannula was slowly withdrawn 3 minutes after the drug was delivered and the skin was closed with surgical staples. The rats were sacrificed by cervical dislocation 6 hours after microinjection. The brain was quickly removed and frozen in hexane at −35°C, then stored in a −70°C freezer for further processing.

Tumor Implantation and Subsequent Stereotactic Microinjection of [³H]BCNU into Tumor Site

The 9L glioma was propagated as a solid tumor in the flanks of the rats. For intracranial implantation, tumor fragments were trimmed to approximately 1 × 1 × 1 mm. Fisher 344 male rats were anesthetized as described above. A 3-mm burr hole was drilled 5 mm posterior to the bregma and 3 mm lateral from the sagittal suture. The dura was opened sharply in a cruciate fashion and the cortex aspirated to expose the higher vascular sulcus between the thalamus and the superior colliculus. The bleeding was allowed to subside spontaneously, and the tumor fragment was then implanted into the brain defect. The wound was thoroughly irrigated and the skin closed with surgical staples.

On the 5th day after tumor implantation, the skin was reopened, and the cannula of the 5-μl microsyringe was introduced into the tumor at a depth of 2 mm. The delivery of [³H]BCNU was initiated 5 minutes after the cannula was fully inserted. Each rat received a total volume of 2 μl (8 μCi) which was drawn from a solution containing 3.7 or 4.6 mg [³H]BCNU in 27.7 or 34.5 μl of 95% ethanol solution. This was also administered at a rate of 0.2 μl/min which was controlled by the same microinjection unit. The cannula was withdrawn 5 minutes after the drug was delivered and the skin was closed with surgical staples. The rats were sacrificed and their brains removed 6 hours after the microinjection.

Surgical Implantation of the Polymer in Normal Brain

Surgical implantation of polymer containing [³H]BCNU was performed in non-tumor-bearing animals. A slit 3 to 5 mm deep was made in the dura and brain parenchyma with a No. 11 scalpel blade. The p(CPP:SA) polymeric disc was inserted into the brain parenchyma with a pair of forceps until it was no longer visible. Once the bleeding spontaneously ceased, the skin was closed with surgical staples. Rats receiving [³H]BCNU-containing polymers were sacrificed 1 (n = 3), 3 (n = 3), 7 (n = 3), 14 (n = 2), and 30 (n = 2) days following surgical implantation, and the brain was prepared for analysis as described above.

Preparation of Tissues for Quantitative Autoradiography

The frozen brain was mounted on a cryostat chuck with O.C.T. embedding medium (Miles Inc., Elkhart, IN) and cut into 20-μm coronal sections using a cryomicrotome (Microm, Heidelberg, Germany) at −20°C. Every tenth section was collected on a glass slide, so that the total distance between sections was 200 μm, and the slides were placed in an x-ray cassette that contained [³H]-sensitive autoradiography film (LKB Ultrofilm, Leica, Deerfield, IL or Hyperfilm, Amersham, Arlington Heights, IL). In addition to the brain sections, a commercially-prepared tritium microscale (Amersham, Arlington Heights, IL) with eight different premeasured activities was placed within the cassette. The autoradiography film was exposed for 2 weeks at room temperature. The film was then developed for 5 minutes at about 22°C (D-19 developer), immersed for 30 seconds in a stop bath (for Leica Ultrofilms only), 5 minutes in fixer, and 20 minutes in filtered flowing water at 22°C, and allowed to dry (all solutions from Eastman Kodak Company, Rochester, NY).

Analysis of Autoradiography Films

Previously developed autoradiographic films were placed on a light box and digitized to produce digital images that were 512 × 512 pixels with 256 gray levels. The tritium radioactivity at each pixel location was determined by comparing the pixel intensity to a standard curve obtained from digital images of tritium-labeled standards, which were reproduced on each film and digitized identically to the brain sections. The radioactivity due to free BCNU was expected to be ~10% of the total radioactivity (see Discussion (30)). The program NIH Image was used to measure concentration profiles from individual digital images. Concentration profiles at close proximity to the center of the injection or implantation site were determined

directly from digital images by scanning the image from the center of the injection site or the edge of the polymer to the periphery of the brain section. Concentration profiles were compared to mathematical models described in the next section.

For images obtained from animals receiving polymer implants, the total mass of drug present in each coronal section on the anteroposterior axis at each time point was also measured. The total drug mass present in brain parenchyma, subarachnoid space and the entire brain section was determined by integrating the local concentration measured for each pixel location over the selected region of the section. Assuming that the density of the tissue within each region is constant, we have

$$M_T = \rho \sum_{i,j} C_{ij} \cdot \Delta V \tag{1}$$

where M_T is the total mass present in the selected area, ρ is the density of the tissue (~ 1 g/cm^3), C_{ij} is the local concentration at pixel location (i,j), and ΔV is the volume of the selected region within the section. ΔV was obtained by measuring the dimensions of a single pixel, counting the number of pixels in the selected region, and multiplying the area of the total selected region by the thickness of each section (20 μm). Noting that the distance between adjacent sections is 200 μm (ten times the thickness of section), the drug distribution on the anteroposterior axis was quantified, and the extent of distribution was calculated. The extent of distribution was defined as the distance from the most anterior section with activity significantly higher than (greater than two standard deviations above) the background level to the most posterior section with activity significantly higher than the background level.

DATA ANALYSIS

In Vitro Release

As noted in a previous study (10), and confirmed here, p(CPP:SA) implants did not erode significantly during the first day of incubation in phosphate-buffered saline solution at 37°C. Thus, on the first day, the in vitro release kinetics of [^{3}H]BCNU from the p(CPP:SA) pellet can be described by a model for a diffusional release from a monolithic polymer pellet. Assuming a spherical geometry, the rate of release of BCNU is related to time as follows (11):

$$\frac{M_t}{M_0} = 6\sqrt{\frac{D_{eff} \cdot t}{\pi \cdot a^2}} - \frac{3D_{eff}t}{a^2} \quad \text{for} \quad \frac{M_t}{M_0} < 0.4 \tag{2}$$

where M_0 is the initial mass of BCNU in the polymer, M_t is the mass of BCNU released from the polymer at time t, a is the equivalent radius of the implant, and D_{eff} is the effective diffusion coefficient of the drug in the polymeric device.

Models for the Transport of BCNU in the Rat Brain

Brain tissue can be modeled as three phases: extracellular space (ECS), intracellular space (ICS), and cell membranes (CM) (12). Thus, the number of moles of BCNU per total brain volume, C, can be expressed as:

$$C = \alpha \cdot C_{ecs}^0 + \beta \cdot C_{ics}^0 + (1 - \alpha - \beta) \cdot C_{cm}^0 \tag{3}$$

where α and β are the volume fractions of ECS and ICS, respectively, and C_{ecs}^0, C_{ics}^0, and C_{cm}^0 indicate the moles of BCNU

per phase volume, which are defined following the volume-averaging approach of Nicholson (12). In general, the fate of a drug delivered to the brain depends on rates of transport (via diffusion and fluid convection), elimination (by degradation, metabolism and permeation through blood capillaries), and local binding or internalization (Figure 1). If we assume the brain tissue is isotropic, the local concentration of drug molecules in the brain can be described by the following partial differential equation, which quantifies transport and elimination in the brain:

$$\frac{\partial C}{\partial t} = -\nabla \cdot (-\alpha \cdot {}_{ecs}\nabla C_{ecs}^0 + \alpha \cdot \bar{v}_r C_{ecs}^0) - (\alpha \cdot k_{ecs} \cdot {}_{ecs}^0$$

$$+ \beta \cdot k_{ics} \cdot C_{ics}^0 + (1 - \alpha - \beta) \cdot k_m \cdot C_{cm}^0) - \frac{\partial B}{\partial t} \tag{4}$$

where the total concentration of bound drug B is defined by analogy to Equation 3 (B = $\alpha \cdot B_{ecs}^0 + \beta \cdot B_{ics}^0 + (1 - \alpha - \beta) \cdot B_{cm}^0$). Equation 4 can be combined with Equation 3 and reduced to:

$$\underbrace{\frac{\partial C_{ecs}^0}{\partial t}}_{\text{transient}} + \underbrace{\frac{\alpha}{\alpha^*} \bar{v}_r \cdot \nabla C_{ecs}^0}_{\text{convection}} = \underbrace{\frac{\alpha}{\alpha^*} D_{ecs} \nabla^2 C_{ecs}^0}_{\text{diffusion}}$$

$$\underbrace{- \frac{\alpha \cdot k_{ecs} + \beta \cdot k_{ics} \cdot P_{i:e}}{\alpha^*} C_{ecs}^0}_{\text{elimination}} \tag{5}$$

with

$$\alpha^* = \alpha \cdot (1 + K_{ecs}) + \beta \cdot P_{i:e} \cdot (1 + K_{ics})$$

$$+ (1 - \alpha - \beta) \cdot P_{m:e} \tag{6}$$

where t is the time following implantation, K_{ecs} is the binding constant between bound and free BCNU in ECS ($K_{ecs} = B_{ecs}^0/C_{ecs}^0$), K_{ics} is the binding constant between bound and free BCNU in ICS ($K_{ics} = B_{ics}^0/C_{ics}^0$), $P_{i:e}$ is the partition coefficient between ICS and ECS ($P_{i:e} = C_{ics}^0/C_{ecs}^0$), $P_{m:e}$ is the partition coefficient between phase CM and ECS ($P_{m:e} = C_{cm}^0/C_{ecs}^0$), $\bar{v}_r$ is a vector describing the fluid velocity, D_{ecs} is the diffusion coefficient of the drug in the ECS, and k_{ecs}, k_{ics} are first-order elimination constants in ECS and ICS, respectively. In obtaining Equation 5, we assumed: (i) BCNU is neither eliminated nor bound in the membrane phase; (ii) the concentration of bound BCNU is directly proportional to the concentration of free BCNU in both ECS and ICS; (iii) BCNU is eliminated by first-order processes in both ECS and ICS; (iv) local equilibrium is achieved between the ECS, ICS, and CM phases. This last assumption is reasonable since the characteristic time for BCNU diffusion through ECS ($t_D \sim L_{cell}^2/D_{ecs} = (10 \mu m)^2/(14.3 \times 10^{-6} cm^2/s) = 0.07$ s; $L_{cell} = $ cell dimension (13)) is much larger than the characteristic time for permeation through cell membranes ($t_M \sim L_{mem}/k_{mem} = (5 nm)/(0.007 cm/s) = 7 \times 10^{-5}$ s; $L_{mem} = $ plasma membrane thickness, and $k_{mem} = $ permeability coefficient for BCNU through biological membranes (14), based on the octanol:water partition coefficient.); $t_D \approx 1000 t_M$. If we use the definitions of total concentration (C) in Equation 3 and partition coefficients ($P_{i:e}$ and $P_{m:e}$), Equation 5, in spherical coordinates, can be expressed as follows:
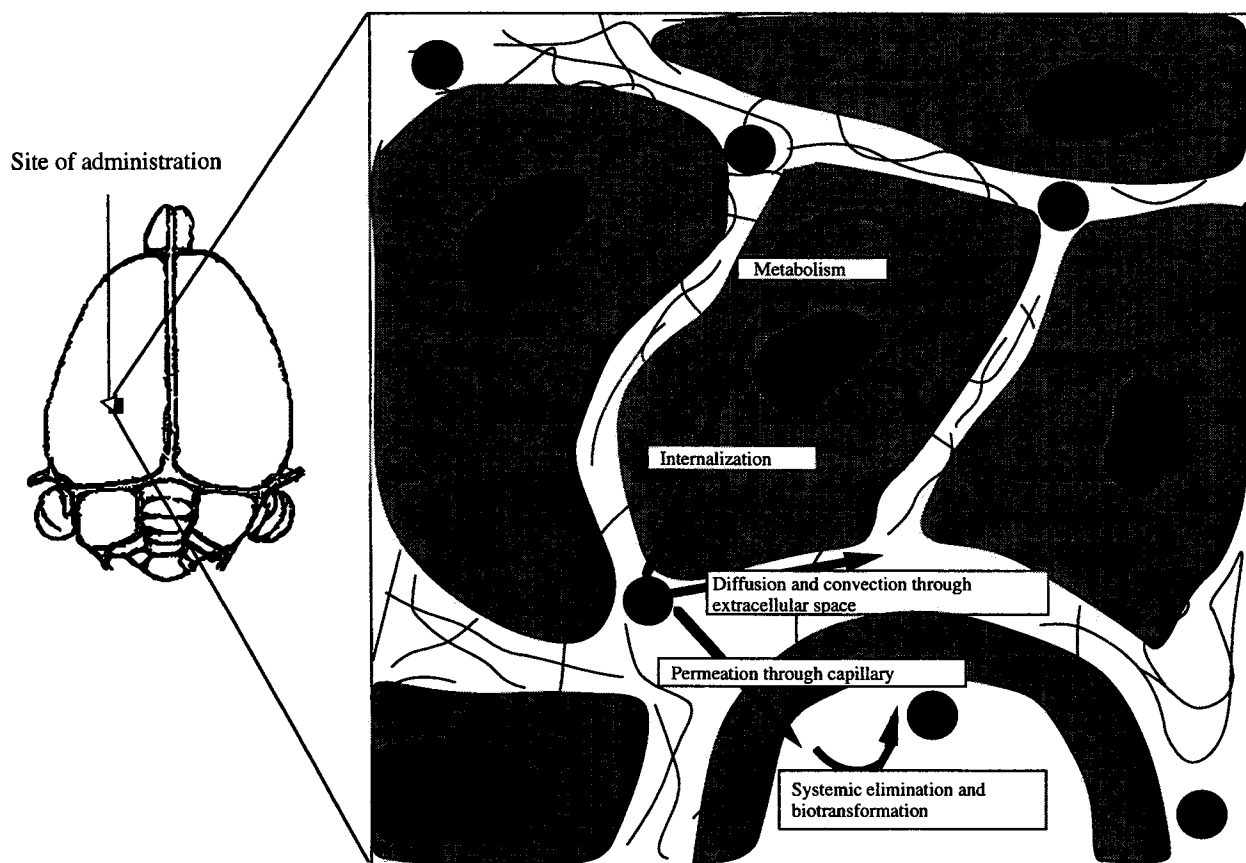
Fig. 1. Mechanisms of BCNU transport and elimination in the brain following administration. The dark circles indicate drug molecules released into the interstitial space.

$$\frac{\partial C}{\partial t} + v \cdot \frac{\partial C}{\partial r} = D \cdot \left[\frac{1}{r^2} \frac{\partial}{\partial r} r^2 \frac{\partial C}{\partial r} \right] - k \cdot C \qquad (7)$$

where v is the apparent radial velocity in the ECS ($v = (\alpha/\alpha^*) \cdot v_r$), D is the apparent diffusion coefficient of the drug in the brain ($D = (\alpha/\alpha^*) \cdot D_{ecs}$), r is the radial distance from the center of the polymer, and k is the apparent first-order elimination constant ($k = (\alpha \cdot k_{ecs} + \beta \cdot k_{ics} \cdot P_{i:e})/\alpha^*$). Note that Equation 7 was obtained directly from Equation 5, since our assumptions lead to a linear relationship between total concentration and extracellular phase concentration: $C = \alpha \cdot C^0_{ecs} + \beta \cdot P_{i:e} \cdot C^0_{ecs} + (1 - \alpha - \beta) \cdot P_{m:e} \cdot C^0_{ecs}$.

Case I—Surgical Implantation of the Polymer in the Normal Brain (Convection Neglected)

Since the height and diameter of the polymer disc were similar, the implant is assumed to have a spherical geometry. Furthermore, a sustained drug concentration in the pellet is assumed. The initial and boundary conditions are: (i) concentration in the brain tissue is zero outside the polymer pellet at the time of insertion of the pellet (Equation 8); (ii) the pellet provides a sustained source of drug, and the concentration of drug at polymer/tissue interface is constant (Equation 9); (iii) concentration of drug far from the polymer pellet is zero (Equation 10).

$$C = 0 \quad \text{for} \quad t = 0; \quad r > a \qquad (8)$$

$$C = C_i \quad \text{for} \quad t > 0; \quad r = a \qquad (9)$$

$$C = 0 \quad \text{for} \quad t > 0; \quad r \rightarrow \infty \qquad (10)$$

where a is the equivalent radius of the polymer implant, and C_i is the concentration of BCNU at the polymer/tissue interface. Assuming steady-state, and applying the two boundary conditions to the governing equation, we obtain (15):

$$\frac{C}{C_i} = \frac{a}{r} \exp\left[-\phi\left(\frac{r}{a} - 1\right) \right] \qquad (11)$$

where ϕ is the diffusion/elimination modulus, $a\sqrt{k/D}$. Concentration profiles for transient diffusion and elimination are obtained by solving Equation 7 with initial and boundary conditions (Equations 8–10):

$$\frac{C}{C_i} = \frac{a}{2r} \cdot \left[\exp\left\{ -(r - a)\sqrt{\frac{k}{D}} \right\} \right.$$

$$\cdot \text{erfc}\left\{ \frac{r - a}{2 \cdot \sqrt{D \cdot t}} - \sqrt{k \cdot t} \right\} + \exp\left\{ (r - a)\sqrt{\frac{k}{D}} \right\} \qquad (12)$$

$$\left. \cdot \text{erfc}\left\{ \frac{r - a}{2 \cdot \sqrt{D \cdot}} + \sqrt{k \cdot t} \right\} \right]$$

Case II—Surgical Implantation of the Polymer in the Normal Brain (Convection Included)

In a few cases, the effect of fluid flow in the brain was estimated. The initial and boundary conditions are the same as Case I. However, the convection term is retained in the transport equation (Equation 7). The solution for this partial differential equation, subject to conditions 8–10, is:

$$\frac{C}{C_0} = \frac{a}{2r}\left\{ erfc\left(\frac{r - a - v\cdot t}{2\sqrt{Dt\cdot}}\right) + exp\left(\frac{(r - a)\cdot v}{D}\right) \right.$$

$$\left. \cdot erfc\left(\frac{r - a + v\cdot t}{2\sqrt{D\cdot t}}\right)\right\} \cdot exp(-k\cdot t) \quad (13)$$

To use our mathematical model to analyze experimental data, the values of several parameters must be known or estimated:

1. Volume fractions in the brain were estimated based on the previous literature (12): $\alpha = 0.20$ and $\beta = 0.65$.

2. The partition coefficient between ICS and ECS was assumed to be one ($P_{i:e} = 1$) since both phases were aqueous phases; the partition coefficient between CM and ECS was approximated ($P_{m:e} = 10$) based on measured partition coefficient for BCNU between silicone oil and water (16).

3. BCNU elimination constant in ECS was assumed to be due primarily to transcapillary transport ($k_{ecs} \approx$ ln $2/t_{1/2,transcapillary} =$ ln $2/48$ s $= 0.014$ s^{-1}; $t_{1/2,transcapillary}$ is the extracellular fluid-transcapillary half-time (17)), while BCNU elimination constant in ICS was approximated from the half-time in brain homogenates ($k_{ics} \approx$ ln $2/t_{1/2,degradation} =$ ln $2/110$ min $= 1.05 \times 10^{-4}$ s^{-1}; $t_{1/2,degradation}$ is degradation half-time of BCNU in dog brain homogenates (18))

4. Binding constants were estimated ($K' = K_{ecs} \approx K_{ics} \approx 4.99$) as described in the appendix.

With these parameters, we obtain the conversion factor between C_{ecs}^0 and C from Equation 3: $C = 2.4 \times C_{ecs}^0$. Comparing Equations 11 and 12 with experimental concentrations by least-square method, we estimated the steady-state and transient diffusion/elimination moduli, $\phi = a\sqrt{k/D}$. The interstitial velocity was predicted by using these values and comparing the experimental concentrations at day 1 with Equation 13.

RESULTS

In Vitro Release Study

During incubation in phosphate-buffered saline, [³H]BCNU was continuously released from the 20%-loaded p(CPP:SA) polymer over a 12-day period (Fig. 2a). The release was linear with respect to the square root of time for the first 24 hours (Fig. 2b), with ~50% of the encapsulated drug released in the first 8 hours and ~84% released in 24 hours. The effective diffusion coefficient for BCNU in the polymer (D_{eff}) was estimated by comparing Equation 2 to the amount of BCNU released as a function of time: D_{eff} was found to be 2.0×10^{-8} cm²/s.

Stereotactic Microinjection in Normal Rat Brain and Tumor Site

The spatial distribution of [³H]BCNU in the normal and tumor-bearing rat brains after direct intracranial stereotactic

microinjection was detected from the [³H]-sensitive autoradiographic films (Fig. 3a).. The local concentration of [³H]BCNU at the position of interest on a coronal section was determined from the intensity of exposure at the corresponding position on the autoradiographic film by comparison to a standard curve obtained from the images of ³H microscales exposed on the same film. The concentration profiles within both normal brain tissue and transplanted tumor were similar 6 hours following microinjection (Fig. 4), suggesting that the transport of BCNU in both cases was also similar. Similar results were obtained at 24 hours after injection (data not shown). Because of the similarity in transport after injection, all subsequent experiments with polymer implants were performed in normal rats; this approach permitted analysis of BCNU transport over a long period, which was not limited by the survival of tumor-bearing animal.

Surgical Implantation of the Polymer in the Normal Rat Brain

The distribution of [³H]BCNU in the brain tissue after polymer implantation was observed from the [³H]-sensitive autoradiographic films (Fig. 3b). The distribution of BCNU was quantified by (i) measuring the total amount of drug in each brain section and (ii) measuring the local concentrations in the vicinity of the implantation site.

Total Drug Mass in Each Section

The total amount of drug in each coronal section was determined and tabulated as a function of anteroposterior location (Fig. 5). The peak ³H activity (i.e. the total amount of radioactivity detected within the 20-μm section) was highest at day 1, and it decreased from ~1.3 pCi/section at day 1 to ~0.02 pCi/section at day 30. To quantify the spread of radioactivity on the anteroposterior axis as a function of time, the extent of distribution was calculated (See Methods, Table I). At day 1, 3, and 7, the extent of distribution was similar (~5.4 to 5.8 mm), but decreased slightly at day 14 (4.8 mm), and day 30 (3.6 mm).

A significant amount of activity was observed near the polymer implant and at the periphery of the brain section. We assumed that the activity at the periphery corresponded to the drug within the subarachnoid space (SAS). To differentiate the amount of drug in these two locations, the total activity in the parenchyma (primarily due to drug near the polymer) and the entire brain section (due to both drug near the polymer and drug at the periphery) were measured, and the mass of drug within the two regions was determined separately. The mass of drug contained in the SAS was calculated by subtracting the mass present in the entire brain section by that in the parenchyma (Fig. 6). The drug was generally observed in the SAS only in the sections that bisected the polymer pellet. On the first day, the fraction of drug mass present in SAS was comparable to that in the brain parenchyma. The relative amount of drug present in SAS decreased with time; a significant fraction (~42%) was measured for day 1, but much lower fractions (<12%) were found at days 7 to 30.

Local Concentration Profiles

Local concentration profiles in brain tissue were also measured on individual coronal sections bisecting the polymer
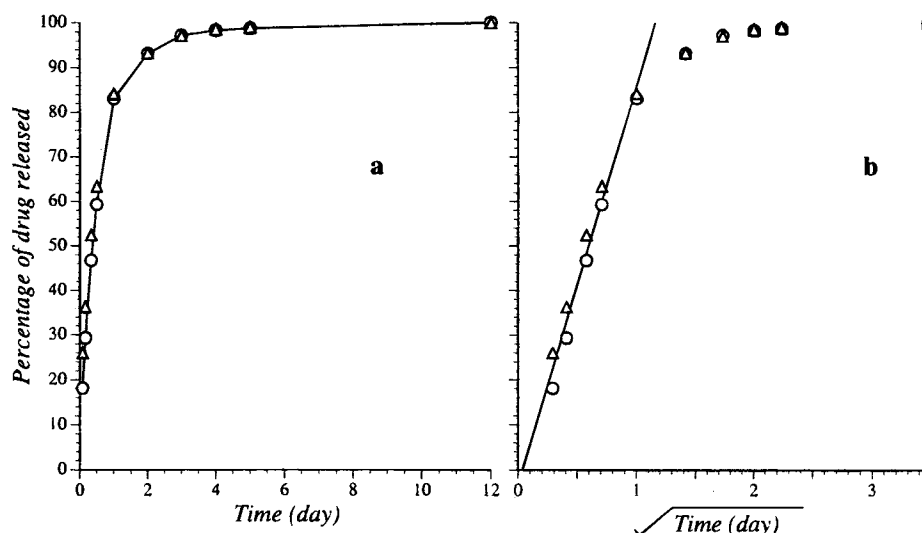
Fig. 2. BCNU release into a well-stirred reservoir. Each symbol represents the cumulative amount of BCNU released for two identical polymer pellets. The cumulative mass released is plotted versus time (a) and the square root of time (b). The slope of the curve in (b) at early time points was determined from the linear regression line.

(Fig. 7 and Table I). Except for the first day, the concentration of BCNU at the polymer/tissue interface remained nearly constant with time. On the first day, the concentration of BCNU at the interface ($\sim$70 pCi/mg, which corresponds to $\sim$1.9 mM, see Discussion) was 2 times greater than at later times ($\sim$30 pCi/mg or $\sim$0.8 mM). The penetration distance of the drug was obtained by scanning the image from the edge of the polymer implant, and identifying the radial position where the concentration had dropped to 10% of the concentration at the polymer/tissue interface (Table I). A dramatic drop in penetration distance was observed between the first and third day, but penetration remained reasonably constant after day 3 ($\sim$1.2 mm).

DISCUSSION

BCNU is known to have high lipophilicity and low ionization at physiologic pH (19, 20); its rate of diffusion through water (1.43×10^{-5} cm^2/s) has been measured previously. In our experiments, [^{3}H]BCNU was slowly released from p(CPP:SA) polymer pellets immersed in phosphate-buffered saline. The rate of diffusion from the polymer pellet ($D_{eff} = 2 \times 10^{-8}$ cm^2/s) is consistent with penetration through an undegraded p(CPP:SA) phase. When identical pellets were implanted in animals, high concentrations of radioactivity were found in the brain tissue surrounding the implant.

The BCNU concentration profiles within both normal rat brains and experimental tumors in rat brains following microinjection were similar (Fig. 4), suggesting that the transport and elimination of the drug were comparable in both cases. The similarity between normal and tumor-bearing brain suggests that results from transport studies performed in normal rat brains may provide insight into transport within the neoplastic brains. It is important to realize, however, that the present study used tumors propagated in the flank of rats, which may be substan-

tially different from tumors that arise spontaneously. In addition, microinjection was performed 5 days after tumor implantation, and the time course of the biological properties of the tumor in relation to the diffusion and elimination of BCNU is not well understood. Differences in the transport of molecules in tumors, when compared to normal tissue, arise from their heterogeneous blood supply, elevated interstitial pressure, fluid loss from periphery, large distances in the interstitium, heterogeneous binding, metabolism (21) and increased blood-brain barrier permeability (22, 23). In our study of microinjection in tumor, these factors did not appear to influence BCNU transport, perhaps due to our early intervention in the development of glioma. Still, these experiments provide the best available experimental evidence on BCNU transport in normal brain versus tumors, and suggest that differences between the two situations are minimal.

Concentration profiles measured one day after polymer implantation were different from concentration profiles at later times, since BCNU appeared to be transported a greater distance from the polymer at early times (Table I and Fig. 7). Before the polymer pellet was inserted in the brain, an incision was made in the brain parenchyma. Surgical incision in the brain causes injury to the cerebral vessels resulting in their increased permeability, which allows serum constituents into the ECS, resulting in vasogenic edema (24). This condition causes the ECS to dilate, and sets up a hydrostatic pressure gradient from the site of edema to the ependyma. Since the extracellular space is in direct communication with the ventricular cerebrospinal fluid (CSF), the hydrostatic pressure differential between the interstitial fluid in the edematous tissue and the CSF drives the movement of edema fluid into the CSF (25). This is consistent with our experimental findings, especially for the first day after polymer implantation: insertion of the polymer appears to cause local edema, and increased fluid movement within the ECS carries the drug from the polymer site to the ventricular system.
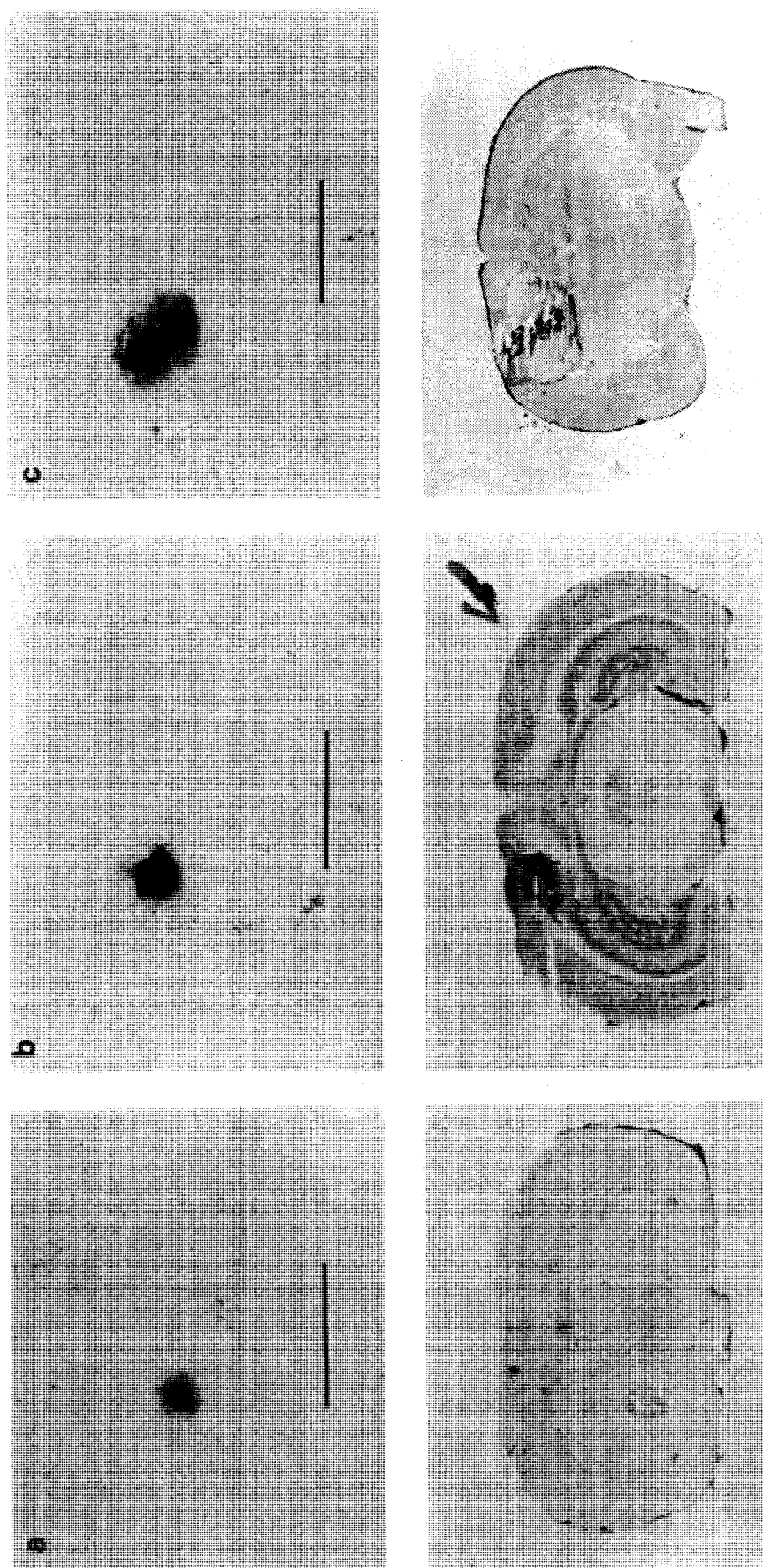
Fig. 3. Autoradiographs (top panels) obtained from coronal sections (bottom panels) of normal rat brains. Darker areas on the autoradiographs represent higher tritium activity and lighter areas represent lower tritium activity. Panel a shows a section obtained 6 hours following stereotactic microinjection of [³H]BCNU in a normal rat brain. Panel b shows a section obtained 6 hours following stereotactic microinjection of [³H]BCNU in a 9L glioma-transplanted rat brain. Panel c shows a section, which bisects the polymer implant, obtained 14 days following implantation of a [³H]BCNU-loaded polymer pellet. The lengths of the black bars at the bottom of the top panels correspond to an actual length of 5 mm.
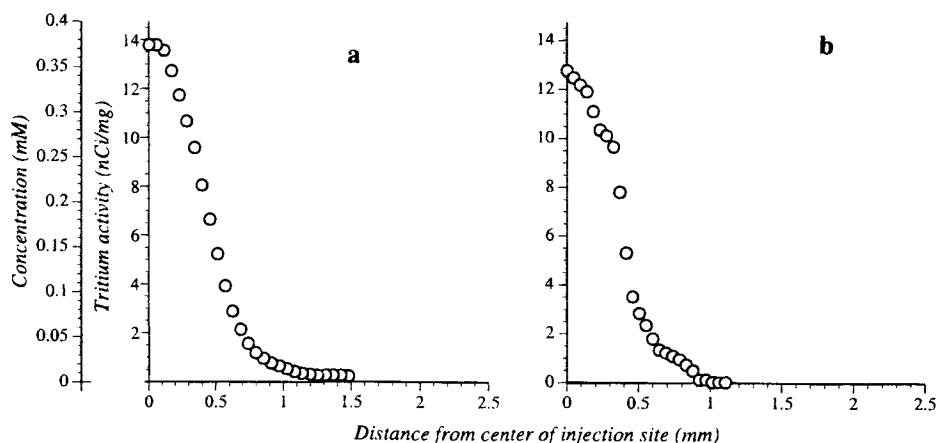
Fig. 4. Concentration profiles of [³H]BCNU at the site of microinjection. Position of the symbols were determined by scanning individual coronal sections and determining the concentration as a function of distance from the edge of the polymer at 6 hours for (a) normal brain, and (b) tumor-bearing brain.

This increased fluid convection caused deeper penetration of drug into the parenchyma (as observed in Fig. 7 a), and increased accumulation of drug in the SAS (as observed in Fig. 6a). Our experiments suggest that this vasogenic edema following trauma in rat brain resolves between days 1 and 7, consistent with previous studies (26).

The concentration profiles were compared with the steady-state solution to the diffusion/elimination equation (Equation 11) to obtain the diffusion/elimination modulus, ϕ (Table I). Except for the measurement obtained at day 1, the ϕ values were similar, with an average value of 2.7. Using the transient solution to the diffusion/elimination equation (Equation 12), the ϕ was calculated to be 2.1. Assuming $D_{ecs} \approx D_{agar} = 14.3 \times 10^{-6}$ cm²/s (17), and using our estimated parameters ($k_{ecs} = 0.014$ s⁻¹, and $k_{ics} = 1.05 \times 10^{-4}$ s⁻¹), we calculated the apparent diffusion coefficient, apparent elimination constant and diffusion/elimination coefficient: $D = 4.3 \times 10^{-7}$ cm²/s, $k = 4.4 \times 10^{-4}$ s⁻¹, and $\phi = 4.8$. The diffusion/elimination moduli calculated from the steady-state and transient models (2.7 and 2.1) are in reasonable agreement with our best estimate of ϕ (4.8).

We observed deeper tissue penetration 1 day after polymer implantation than at any subsequent time (Fig. 7). To determine whether this observation could be accounted for by fluid movement in the ECS, appropriate parameters were used ($D = 4.31 \times 10^{-7}$ cm²/s and $a = 1.5$ mm), and the mathematical model (Equation 13) was compared with measured concentration profiles by changing the interstitial fluid velocity and minimizing mean-squared error. The interstitial fluid velocity was estimated to be 3.4 ± 1.7 mm/day, which corresponds to an interstitial velocity, v_n, of 110 ± 60 mm/day. This estimate is consistent with previously measured edema fluid velocities induced experimentally (27) or observed in tumors (28).

Since convection seemed to be significant during the first day of delivery, our simplified transport models (Equation 7) were not valid over the entire delivery period. However, for the majority of the experiment (days 3 to 30), the diffusion/ elimination modulus, ϕ, appears to be a reliable indicator of the diffusion/elimination process. The mean steady-state ϕ

was close to the transient ϕ, suggesting that the steady state approximation was valid over much of the period of study. This is consistent with our previous predictions that steady-state will be achieved within a few hours for BCNU delivery (17). The mathematical models can be used to predict concentration of BCNU at positions far away from the polymer/tissue interface where concentrations are too low to be detected by quantitative autoradiography. For example, using a ϕ value of 2.7 and a C_0 value of 10 mM, the concentration of BCNU at a distance of 5 mm from the interface is about 0.2 μM (Equation 11).

In a previous study using similar polymers to deliver BCNU to the brains of rabbits (29), the penetration distance of BCNU was ~1.1 to 1.3 mm for the first 3 days following implantation. In contrast, the penetration distance for rats was higher on the first day, 4.7 mm. The penetration distance in rats observed here dropped to 1.6 mm on day 3, 1.3 mm on day 7 and 1.1 mm on day 14, all similar to the distance observed in rabbits. This suggests that fluid movement during the initial period of BCNU delivery, which we suggest accounts for the enhanced penetration observed on day 1 in rats, was not as significant in the rabbit model. The reason for the difference between rats and rabbits observed during the first day is not clear, but may be related to the susceptibility to edema, the location of implantation and the method of surgery. Using the same mathematical model, data from the rabbit produced a diffusion/elimination modulus of ~2.2 whereas data from the rat yielded a value of about 2.7. This similarity showed the consistency of relative rates of BCNU diffusion and elimination in these animals.

In this study, we measured [³H] activity within the brain to infer BCNU concentrations after administration of [³H]BCNU. Since BCNU is reactive, only a fraction of the measured radio-activity corresponds to intact BCNU. In other experiments, using comparable experimental conditions, we have determined that ~10% of the radioactivity measured in monkey brains after polymer delivery corresponds to BCNU (30); BCNU recovery did not depend on time after implantation or location of sampling in the brain. Therefore, we assumed that 10%
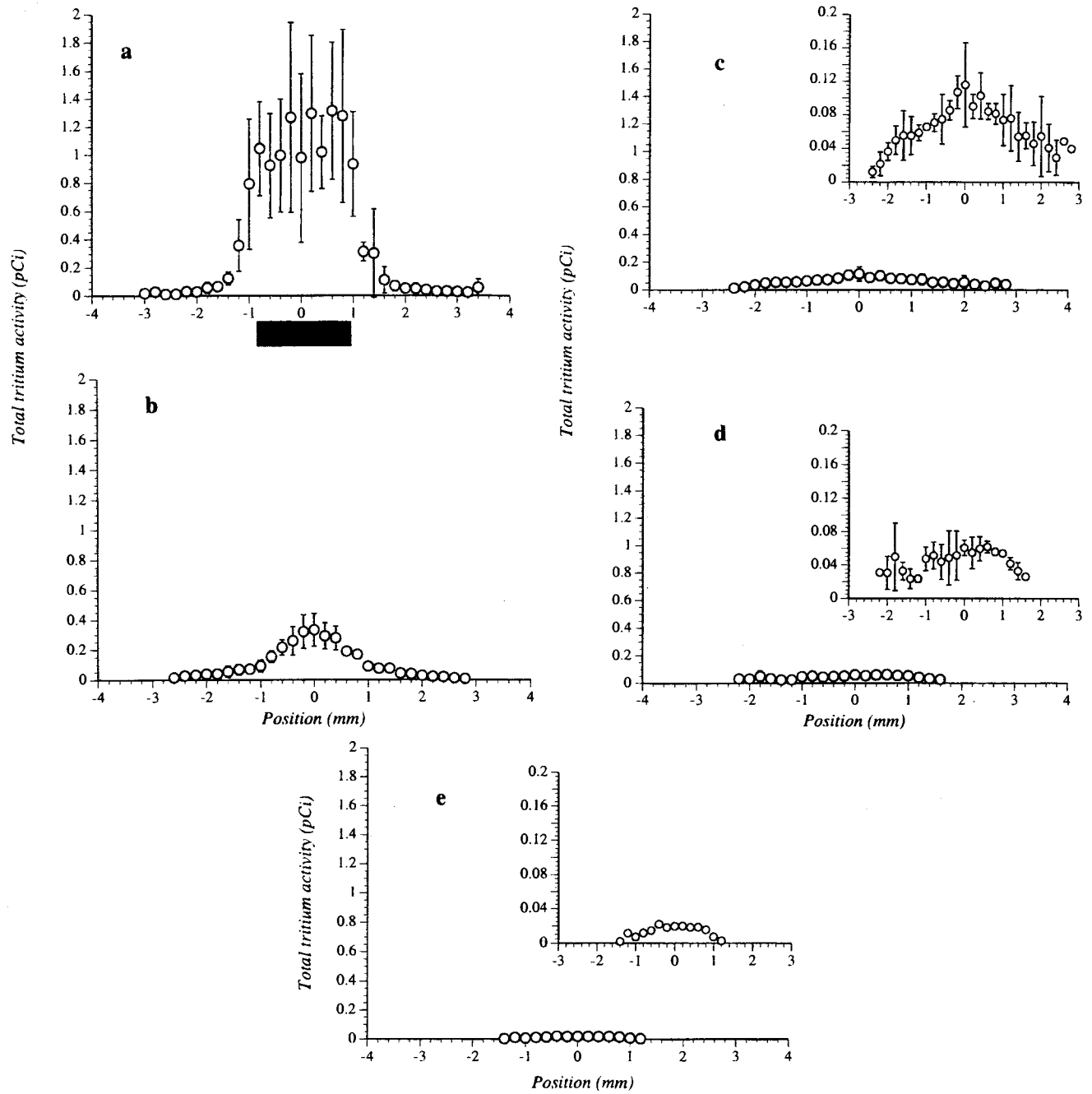
Fig. 5. The total radioactivity within coronal sections of the brain containing a [^{3}H]BCNU-loaded polymer pellet were determined as a function of position from the center of the polymer at (a) 1 day (the penetration distance is out of scale in this plot), (b) 3 days, (c) 7 days, (d) 14 days, and (e) 30 days following implantation. Each symbol represents the total radioactivity in a section, which was calculated by integrating concentrations determined from a digitized autoradiograph. The solid bar below panel (a) indicates the position of the polymer implant. Error bars indicate the strandard deviations for determinations from 3 identically treated animals.

Table I. Summary of BCNU Concentration Profiles in the Rat Brain

Time following implantation (day)	C_o (mM)	d_p (mm)	E.D. (mm)	ϕ
1	1.9 ± 0.4	4.7 ± 1.2	5.8 ± 1.2	—
3	0.94 ± 0.07	1.6 ± 0.6	5.4 ± 0.2	1.6 ± 1.0
7	0.77 ± 0.09	1.2 ± 0.4	5.6 ± 0.5	3.1 ± 2.2
14	0.73 ± 0.03	1.0 ± 0.5	4.8 ± 0.0	3.6 ± 2.0
30	—	—	3.6 ± 0.6	—

Note: The distance for penetration (d_p) was estimated by scanning from the edge of the polymer pellet, and identifying the radial position where the concentration had dropped to 10% of the concentration at the polymer/tissue interface, C_O (see Fig. 7). The extent of distribution (E.D.) was obtained by where the most anterior and posterior sections with activity significantly higher than (>2 standard deviations) the background level were located, and calculating the distance between those sections (see Fig. 5). ϕ is the diffusion/elimination modulus $(a\sqrt{k/D})$, which had an average value of $\phi = 2.7$ from fitting the steady-state equations and value of 2.1 from fitting the transient equations. Each value represents the mean ± standard deviation.

of the radioactivity was due to BCNU in calculating tissue concentrations (Table I, Fig. 4 and 7). The BCNU concentration at the polymer/tissue interface decreased with time (Table I). It is important to note that the peak concentrations measured in this study, 0.7–1.9 mM, are substantially higher than tissue concentrations achieved by other modes of BCNU delivery to the brain. While we define penetration distance as the distance required for BCNU concentration to drop to 10% of this peak value, effective antitumor activity is likely to penetrate much farther in the brain, since BCNU is known to be active at 14–15 μM (31), much lower concentrations than we report near the polymer. Even if our estimate of the fraction of active BCNU (10%) is high, these experiments indicate that cytotoxic levels of BCNU extend at least several mm from the polymer.

In summary, polymer pellets can deliver extremely high doses of BCNU to the brain for a sustained period. Even the present polymer system, which releases BCNU over several days in a common *in vitro* assay system, provides at least 30 days of sustained delivery when implanted in the brain. This sustained delivery depends on the local rates of transport and elimination of BCNU from the brain tissue, as well as the rate of release from the polymer. These results help explain the success of BCNU-loaded polymer in increasing survival in animals with experimental brain tumors and in human brain tumor patients. In addition, these results suggest that the majority of BCNU is confined to a relatively small volume near the polymer ($\sim$1 mm). This limited penetration may influence the efficacy of this therapy, particularly in humans, where tumors may recur a considerable distance from the surgical resection site ($\sim$1 cm). Therefore, we suggest that brain tumor therapy may be enhanced by using other chemotherapy agents that, because of their physical properties, penetrate further into the brain tissue near the polymer. In fact, we have previously reported the use of drug-polymer conjugates which may improve local penetration (32). We expect that improvements in polymer delivery technology, which are based on our under-
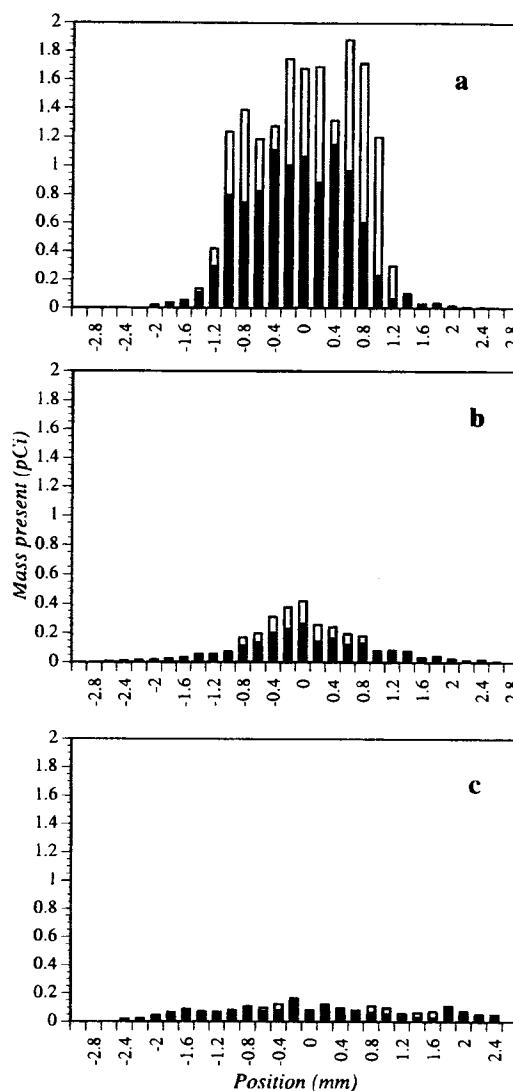

Fig. 6. The total radioactivity within subarachnoid space (white), parenchyma (black) and the entire brain section (white + black) containing a [^{3}H]BCNU-loaded polymer pellet were determined as a function of position from the center of the polymer at (a) 1 day, (b) 3 days, and (c) 7 days following implantation. The total radioactivity within a coronal section was calculated by integrating concentrations determined from a digitized autoradiograph; the radioactivity within the parenchyma was calculated by integrating concentrations that are inside the internal capsule; the radioactivity within the subarachnoid space was determined by taking the difference between the two quantities just described. Each graph represents 1 animal.

standing of the dynamics of drug transport in local tissue, will provide enhanced survival in future pre-clinical and clinical testing.

APPENDIX

Estimation for the Binding Constants

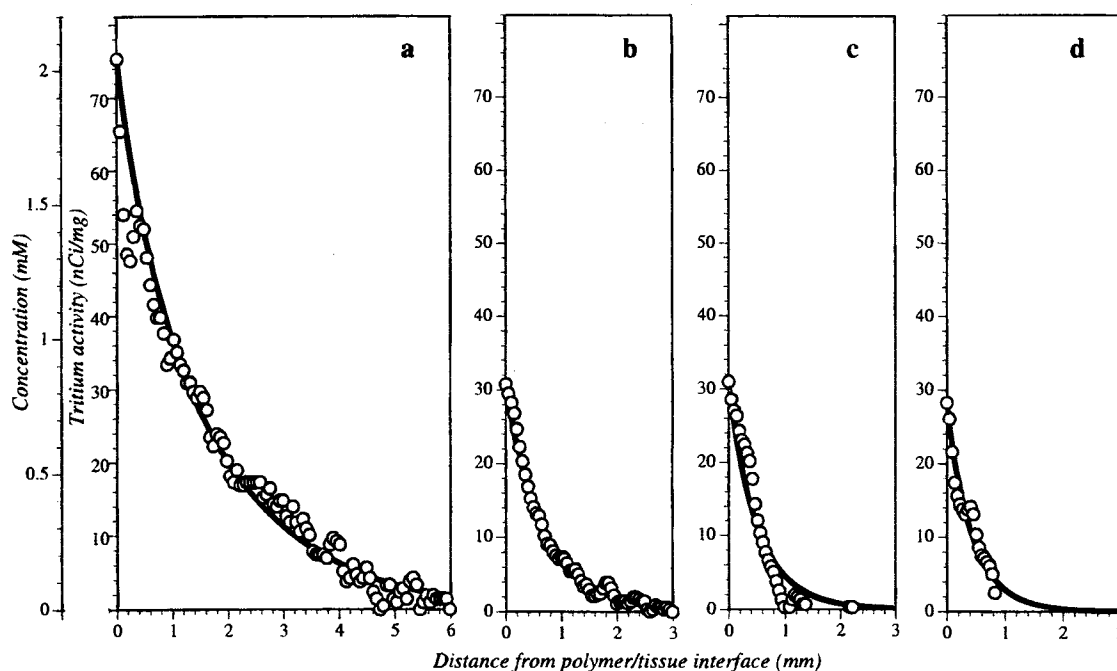$$K = \frac{B}{C} = \frac{46}{26} = 1.77(8)$$

Fig. 7. Concentration profiles in the vicinity of a polymer implant. Position of the symbols were determined by scanning individual coronal sections and determining the concentration as a function of distance from the edge of the polymer at (a) 1 day, (b) 3 days, (c) 7 days and (d) 14 days. The solid lines show the steady-state diffusion/elimination model, in which ϕ was varied to compare most favorably with the experimental data (See Table 1). In addition to the diffusion/ elimination model, Equation 10, panel (a) also contains a dashed line which indicates the best fit to the diffusion/ elimination/convection model, Equation 14. Because of their proximity, it is difficult to distinguish these two curves in the figure.

According to Equation 3,

$$K = \frac{\alpha \cdot B_{ecs}^0 + \beta \cdot B_{ics}^0}{\alpha \cdot C_{ecs}^0 + \beta \cdot C_{ics}^0 + (1 - \alpha - \beta) \cdot C_{cm}^0}$$

$$= \frac{\alpha \cdot K_{ecs} \cdot C_{ecs}^0 + \beta \cdot K_i \cdot P_{i:e} \cdot C_{ecs}^0}{(\alpha + \beta \cdot P_{i:e} + (1 - \alpha - \beta) \cdot P_{m:e}) \cdot C_{ecs}^0}$$

$$K = \frac{\alpha \cdot K_{ecs} + \beta \cdot K_i \cdot P_{i:e}}{\alpha + \beta \cdot P_{i:e} + (1 - \alpha - \beta) \cdot P_{m:e}}$$

Assuming $K' \approx K_{ecs}$

$\approx K_{ics}$, we have

$$K = K' \left[\frac{\alpha + \beta \cdot P_{i:e}}{\alpha + \beta \cdot P_{i:e} + (1 - \alpha - \beta) \cdot P_{m:e}} \right].$$

Therefore, $K' = 4.99$.

NOTATION

Symbols

a   equivalent radius of the polymer
B   mass of bound BCNU per total brain volume
C   mass per total brain volume
C^0_{ecs} mass of BCNU in ECS per ECS volume
C^0_{ics} mass of BCNU in ICS per ICS volume
C^0_m mass of BCNU in membrane per membrane volume
C_i concentration at polymer/tissue interface

C_{ij} local concentration at pixel (ij)
D   apparent diffusion coefficient of BCNU in brain
D_{ecs} diffusion coefficient of BCNU in ECS
D_{eff} in vitro effective diffusion coefficient of BCNU
k   apparent first-order elimination constant
k_{ecs} first-order elimination constant in ECS
k_{ics} first-order elimination constant in ICS
k_{mem} permeability coefficient of BCNU between aqueous and non-aqueous phases
K   binding constant based on total mass per total brain volume
K_{ecs} binding constant in ECS
K_{ics} binding constant in ICS
L_{cell} cell dimension
L_{mem} plasma membrane thickness
M_0 initial mass of BCNU in polymer
M_t mass of BCNU released at time t
M_T total mass present in selected area
$P_{i:e}$ partition coefficient between ICS and ECS
$P_{m:e}$ partition coefficient between CM and ECS
r   radial distance from the center of polymer
R   rate of BCNU elimination from ECS
t   time after implantation or incubation
t_D time constant for diffusion of BCNU in ECS
t_M time constant for permeation of BCNU across plasma membrane
v   apparent interstitial fluid velocity
v_r interstitial fluid velocity

Abbreviations

BCNU   1,3-bis(2-chloroethyl)-1-nitrosourea
CM   cell membrane
CSF·   cerebrospinal fluid
ECS   extracellular space
ICS   intracellular space
p(CPP:SA)   poly[bis-(p-carboxyphenoxy)propane-sebacic acid]
SAS   subarachnoid space

Greek Letters

α volume fraction of ECS
α^* lumped parameter containing α, β, K_{ecs}, K_{ics}, $P_{i:e}$ and $P_{m:e}$
β volume fraction of ICS
ϵ porosity of the brain
ϕ diffusion/elimination modulus
ρ density of brain tissue
ΔV volume of selected region

ACKNOWLEDGMENTS

REFERENCES

1. R. J. Tamargo, J. S. Myseros, J. I. Epstein, M. B. Yang, M. Chasin, and H. Brem. Interstitial chemotherapy of the 9L gliosarcoma: controlled release polymers for drug delivery in the brain, *Cancer Research* 53:329-33 (1993).

2. H. Brem, A. Kader, J. I. Epstein, R. J. Tamargo, A. Domb, R. Langer, and K. W. Leong. Biocompatibility of a biodegradable, controlled-release polymer in the rabbit brain, *Selective Cancer Therapeutics* 5:55-65 (1989).

3. H. Brem, R. J. Tamargo, A. Olivi, M. Pinn, J. D. Weingart, M. Wharam, and J. I. Epstein. Biodegradable polymers for controlled delivery of chemotherapy with and without radiation therapy in the monkey brain, *Journal of Neurosurgery* 80:283-90 (1994).

4. A. Olivi, and H. Brem. Interstitial chemotherapy with sustained-release polymer systems for the treatment of malignant gliomas, *Recent Results of Cancer Research* 135:149-54, 1994.

5. H. Brem, S. M. Mahaley Jr., N. A. Vick, K. L. Black, S. C. Schold Jr., P. C. Burger, A. H. Friedman, I. S. Ciric, T. W. Eller, J. W. Cozzens, and J. N. Kenealy. Interstitial chemotherapy with drug polymer implants for the treatment of recurrent gliomas, *Journal of Neurosurgery* 74:441-6 (1991).

6. F. H. Hochberg, and A. Pruitt. Assumptions in the radiotherapy of glioblastoma, *Neurology* 30:907-11 (1980).

7. A. J. Domb, M. Rock, J. Schwartz, C. Perkin, G. Yipchuk, B. Broxup, and J. G. Villemure. Metabolic disposition and elimination studies of a radiolabelled biodegradable polymeric implant in the rat brain, *Biomaterials* 15:681-8 (1994).

8. S. A. Grossman, C. Reinhard, O. M. Colvin, M. Chasin, R. Brundrett, R. J. Tamargo, and H. Brem. The intracerebral distribution of BCNU delivered by surgically implanted biodegradable polymers, *Journal of Neurosurgery* 76:640-7 (1992).

9. R. J. Tamargo, K. W. Leong, and H. Brem. Growth inhibition of the 9L glioma using polymers to release heparin and cortisone acetate, *Journal of Neuro-Oncology* 9:131-8 (1990).

10. M. P. Wu, J. A. Tamada, H. Brem, and R. Langer. In vivo versus in vitro degradation of controlled release polymers for intracranial surgical therapy, *Journal of Biomedical Materials Research* 28:387-95 (1994).

11. R. Langer. Polymeric delivery systems for controlled drug release, *Chemical Engineering Communication* 6:1-48 (1980).

12. C. Nicholson. Interaction between diffusion and Michaelis-Menten uptake of dopamine after iontophoresis in striatum, *Biophysical Journal* 68:1699-1715 (1995).

13. B. Alberts, D. Bray, J. Lewis, M. Raff, K. Roberts, and J. Watson. *Molecular biology of the cell*, Third edition. Garland Publications, New York (1994).

14. W. R. Lieb, and W. D. Stein. Biological membranes behave as non-porous polymeric sheets with respect to the diffusion of non-electrolytes, *Nature* 224:240-243 (1969).

15. W. M. Saltzman, and M. L. Radomsky. Drugs released from polymers: diffusion and elimination in brain tissue, *Chemical Engineering Science* 46:2429-2444 (1991).

16. H. Chung, F. I. Tolentino, V. N. Cajita, N. Ueno, and M. F. Refojo. BCNU in silicone oil in proliferative vitreoretinopathy: I. Solubility, stability (in vitro and in vivo), and antiproliferative (in vitro) studies, *Current Eye Research* 7:1199-1206 (1988).

17. R. G. Blasberg, C. Patlak, and J. D. Fenstermacher. Intrathecal chemotherapy: brain tissue profiles after ventriculocisternal perfusion, *The Journal of Pharmacology and Experimental Therapeutics* 195:73-83 (1975).

18. P. M. Kanter, H. S. Schwartz, and C. R. West. Functional and chemical markers of PCNU activity, *Cancer Drug Delivery* 1:11-20 (1983).

19. F. M. Shabel, T. P. Johnston, G. S. McCaleb, J. A. Montgomery, W. R. Laster, and H. E. Skipper. Experimental evaluation of potential anti-cancer agents. VII. Effects of certain nitrosoureas on intracerebral L1210 leukemia, *Cancer Research* 23:725-733 (1963).

20. T. L. Loo, R. L. Dixon, and D. P. Rall. The antitumor agent, 1,3-bis(2-chloroethyl)-1-nitrosourea, *Journal of Pharmaceutical Sciences* 55:492-7 (1966).

21. R. K. Jain. Vascular and interstitial barriers to delivery of therapeutic agents in tumors, *Cancer and Metastasis Review* 9:253-66 (1990).

22. P. A. Grabb, and M. R. Gilbert. Neoplastic and pharmacological influence on the permeability of an in vitro blood-brain barrier, *Journal of Neurosurgery* 82:1053-1058 (1995).

23. R. G., Blasberg, D. Groothuis, and P. Molnar. A review of hyperosmotic blood-brain barrier disruption in seven experimental brain tumor models. In: B. B. Johansson, and C. O. H. Widner (eds). *Pathophysiology of the Blood-Brain Barrier*. Elsevier. Amsterdam, 1990, pp. 197-220.

24. I. V. Gannushkina, L. I. Sukhorukova, and M. V. Baranchikova. Dependence of traumatic brain edema on immunologic reactivity against tissue antigens. In: H. M. Pappius, and W. Feindel (eds). *Dynamics of Brain Edema*. Springer Verlag. Berlin/Heidelberg/New York, 1976, pp. 155-160.

25. H. J. Reulen, M. Tsuyumu, A. Tack, A. R. Fenske, and G. R. Prioleau. Clearance of edema fluid into cerebrospinal fluid, *Journal of Neurosurgery* 48:754-64 (1978).

26. M. E. Carey, G. S. Sarna, and J. B. Farrell. Brain edema following an experimental missile wound to the brain, *Journal of Neurotrauma* 7:13-20 (1990).

27. R. Ferszt, S. Neu, J. Cervos-Navarro, and J. Sperner. The spreading of focal brain edema induced by ultraviolet irradiation, *Acta Neuropathologica* 42:223-9 (1978).

28. U. Groger, P. Huber, and H. J. Reulen. Formation and resolution of human peritumoral brain edema, *Acta Neurochirurgica—Supplementum* 60:373-374 (1994).

29. J. F. Strasser, L. K. Fung, S. Eller, S. A. Grossman, and W. M. Saltzman. Distribution of 1,3-bis(2-chloroethyl)-1-nitrosourea (BCNU) and tracers in the rabbit brain after interstitial delivery by biodegradable polymer implants, *The Journal of Pharmacology and Experimental Therapeutics* 275:1647-1655 (1995).

30. L. K. Fung, M. Ewend, A. Sills, E. Sipos, R. Thompson, H. Brem, and W. M. Saltzman. Interstitial delivery of carmustine, 4-hydroperoxycyclophosphamide and taxol from a biodegradable polymer in the monkey brain. In preparation.

31. K. J. Hunter, D. F. Deen, M. Pellarin, and L. J. Marton. Effect of α-difluoromethylornithine on 1,3-bis(2-chloroethyl)-1-nitrosourea and cis-diamminedichloroplatinum(II) cytotoxicity, DNA interstrand cross-linking, and growth in human tumor cell lines in vitro, *Cancer Research* 50:2769-2772 (1990).

32. W. Dang, O. M. Colvin, H. Brem, and W. M. Saltzman. Covalent coupling of methotrexate to dextran enhances the penetration of cytotoxicity into a tissue-like matrix, *Cancer Research* 54:1729-1735 (1994).